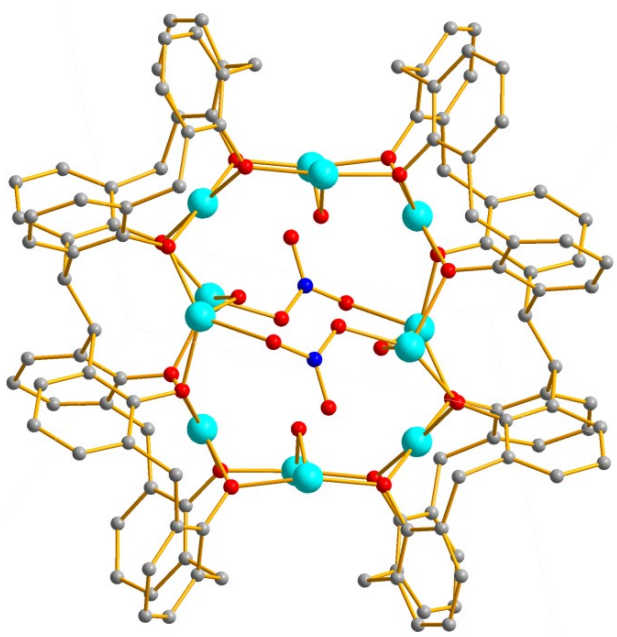

Figure S1. The [Cu_{12}] tetracapped square prism in **4**, highlighting the coordination of the OH^-, L^{8-} and NO_3^- ions.

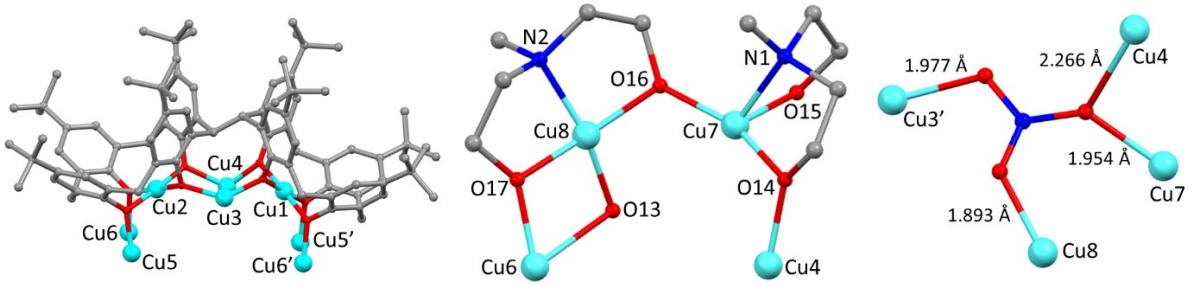

Figure S2. The bonding modes of L (left), Me-dea (middle) and NO_3 (right) in **4**. The latter is μ_3-bridging but with two further contacts to two Cu ions (Cu4, Cu6).

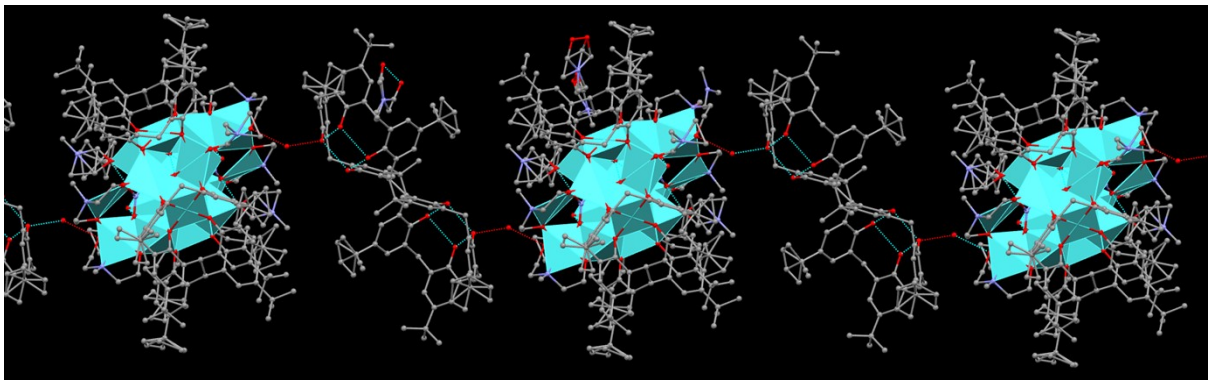

Figure S3. The H-bonded -Cu_{16}-H_2O-H_6L- chains in the crystal structure of **4**. The Cu ions are in polyhedral format and the remaining atoms ball and stick. The H-bonds are shown as dashed lines. H atoms omitted for clarity.

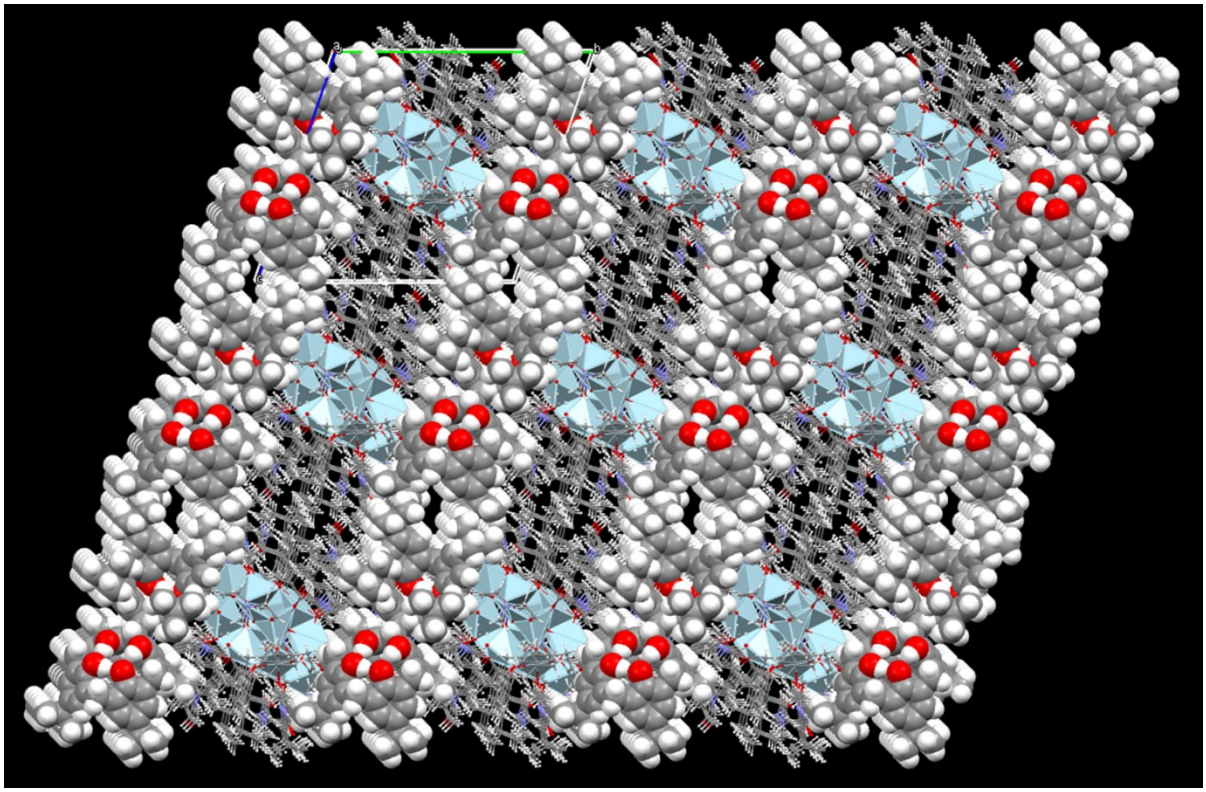

Figure S4. The extended structure in **4** viewed down the *a*-axis highlighting the connection between the cluster in polyhedral format, the H_6L^{2-} counter anions (space fill) and the solvent molecules of crystallisation.

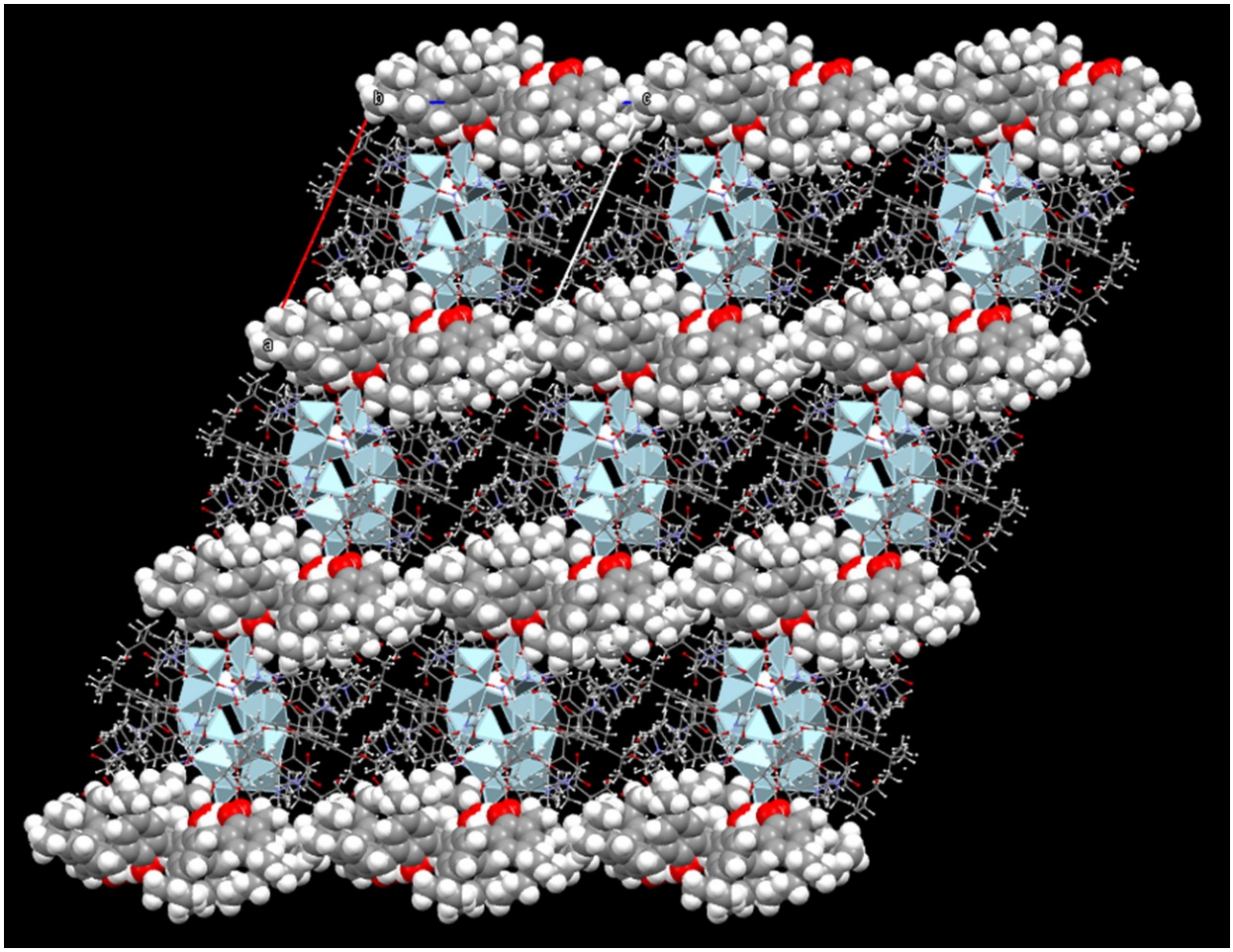

Figure S5. The extended structure in **4** viewed down the *b*-axis highlighting the connection between the cluster in polyhedral format, the H_6L^{2-} counter anions (space fill) and the solvent molecules of crystallisation.

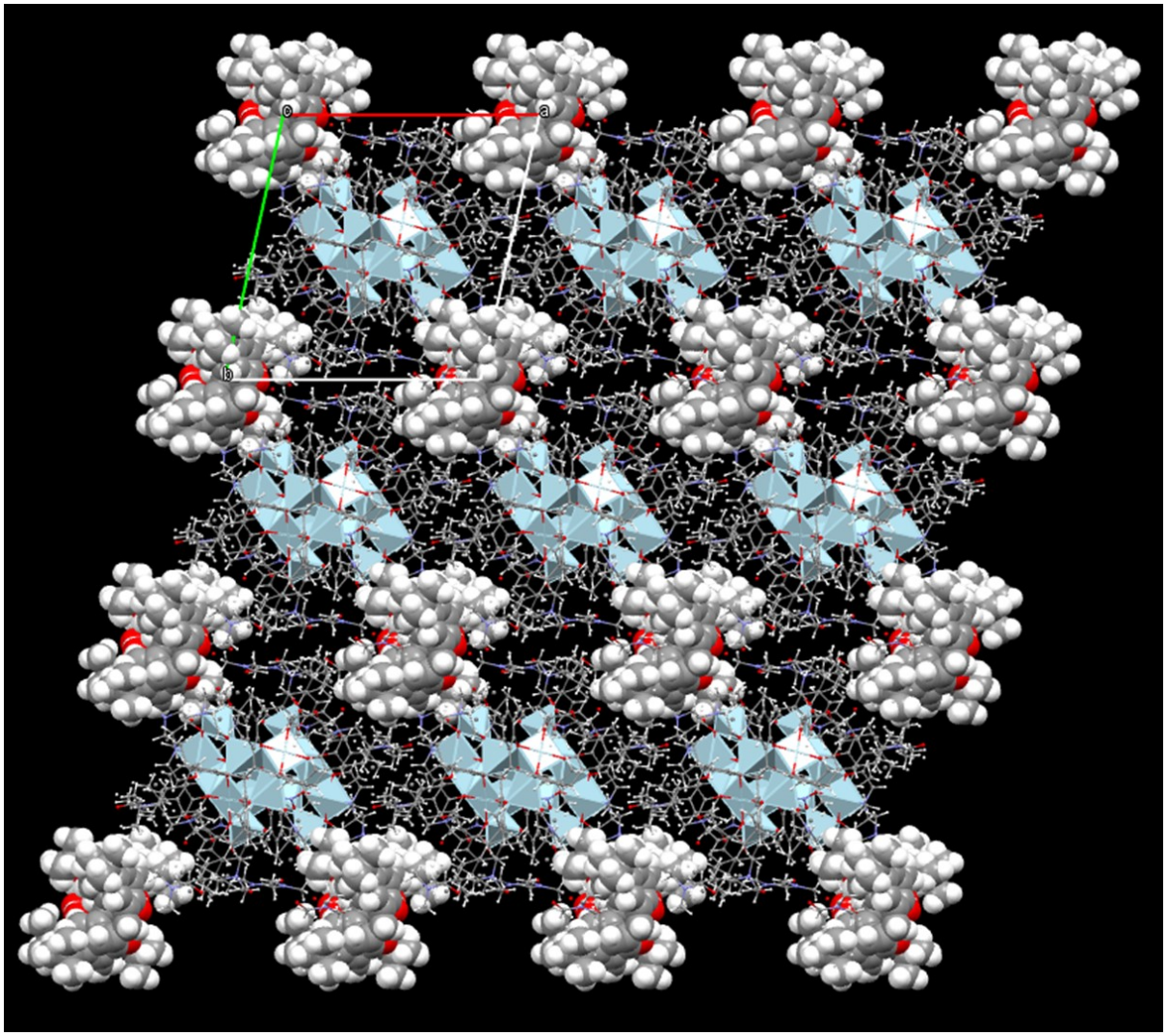

Figure S6. The extended structure in **4** viewed down the *c*-axis highlighting the connection between the cluster in polyhedral format, the H_6L^{2-} counter anions (space fill) and the solvent molecules of crystallisation.

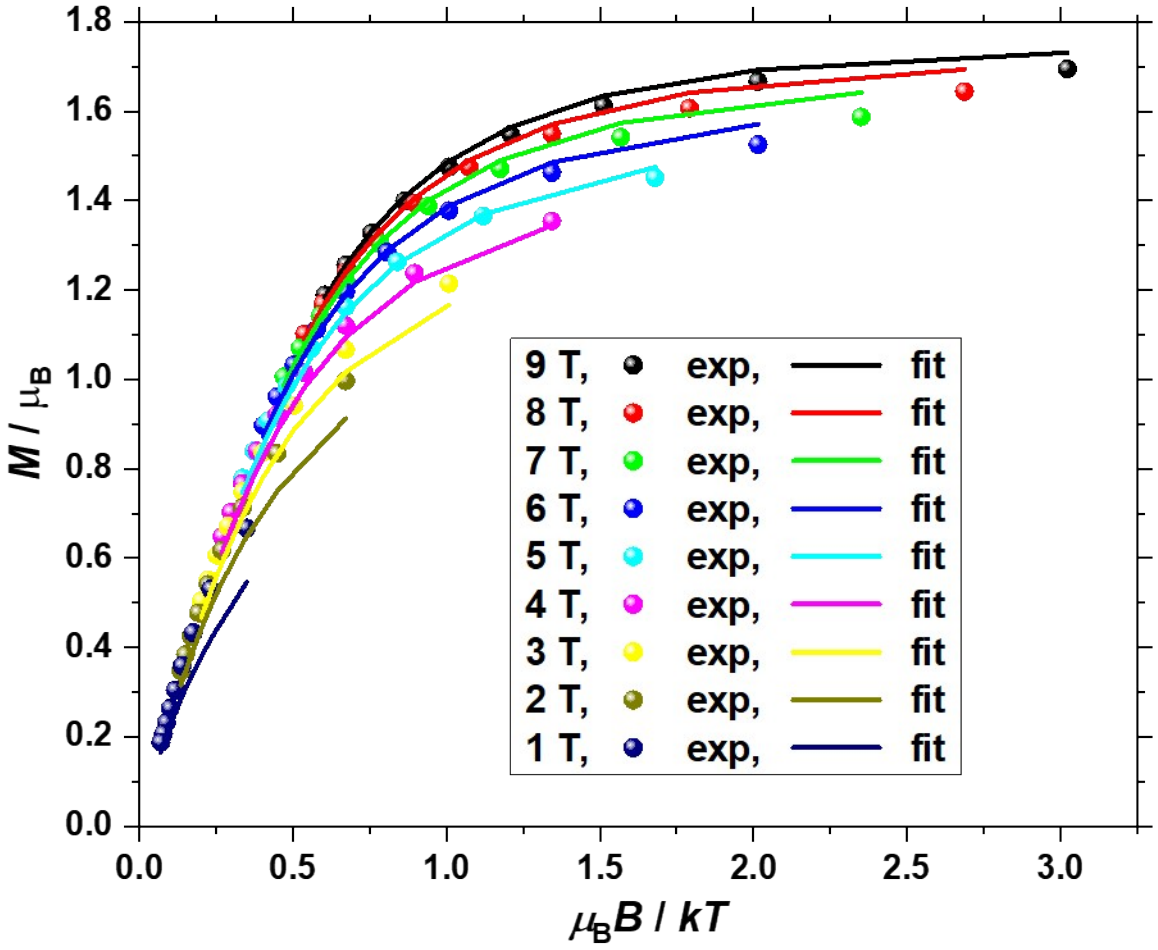

Figure S7. VTVB data of **4** in the temperature range 2 to 10 K and field range 1 to 9 T. The solid lines are a fit of the data assuming an isolated $S = 1$ state, affording $D = -8.5$ cm^{-1} with g fixed to $g = 2.0$ [$\hat{H} = \sum_i D_i(\hat{S}_z^2 - S(S+1)/3)$].

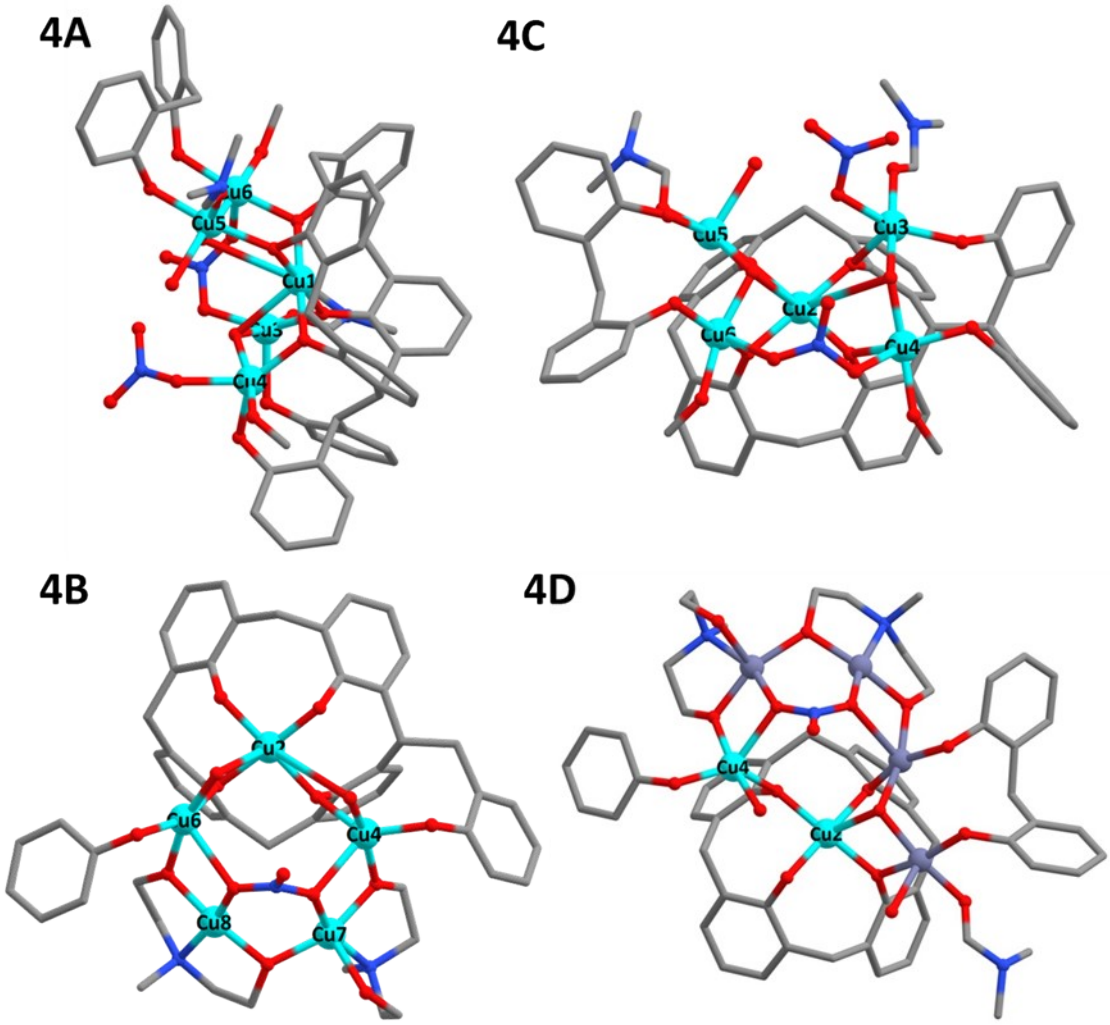

Figure S8. The three pentametallic models **4A**-**C** and the bimetallic model **4D** employed to calculate the magnetic exchange interactions in **4**.

J	cm^{-1}	Avg. Cu-O-Cu Angle (°)	Avg. Cu-O Distance (Å)	Cu-O-Cu-O Dihedral Angle (°)	Cu···Cu Distance (Å)	Bridging group(s)
$J_{Cu1\text{-}Cu3}$	+6.9	95.9	2.108	23.6	3.118	μ-OH, μ-OPh
$J_{Cu1\text{-}Cu4}$	-16.6	101.6	2.091	10.3	3.223	μ_3-OH, μ-OPh
$J_{Cu1\text{-}Cu5}/J_{Cu1\text{-}Cu6}$	-25.3	120.0/120.6	1.962/1.971	--	3.400/3.424	μ-OPh
$J_{Cu2\text{-}Cu3}$	-17.7	119.0	2.038	--	3.514	μ-OPh
$J_{Cu2\text{-}Cu4}$*	-55.7	131.7	2.010	--	3.668	μ-OPh
$J_{Cu2\text{-}Cu5}$	-22.0	102.8	2.087	1.1	3.251	μ-OH, μ-OPh
$J_{Cu2\text{-}Cu6}$	-7.5	100.2	2.081	16.4	3.183	μ-OH, μ-OPh
$J_{Cu3\text{-}Cu4}$	-30.8	125.7	1.957	--	3.482	μ-OH
$J_{Cu4\text{-}Cu7}$	-11.6	103.2	2.014	5.5	3.146	μ-O(NO_2), μ-OR
$J_{Cu5\text{-}Cu6}$	-3.9	107.2	1.947	--	3.135	μ-OH
$J_{Cu6\text{-}Cu8}$	+2.6	98.1	2.049	16.9	3.086	μ-O(NO_2), μ-OR
$J_{Cu7\text{-}Cu8}$	-9.9	114.6	1.930	--	3.249	η^1, η^1, η^2, μ_4-NO_3, μ-OR

*Estimated using bimetallic model **4D**.

Table S2. DFT estimated magnetic exchange interactions alongside the pertinent structural parameters for complex **4**. Calculations are based on the $\hat{H} = -2\sum_{i,j>i} J_{ij}\hat{S}_i \cdot \hat{S}_j$ formalism.

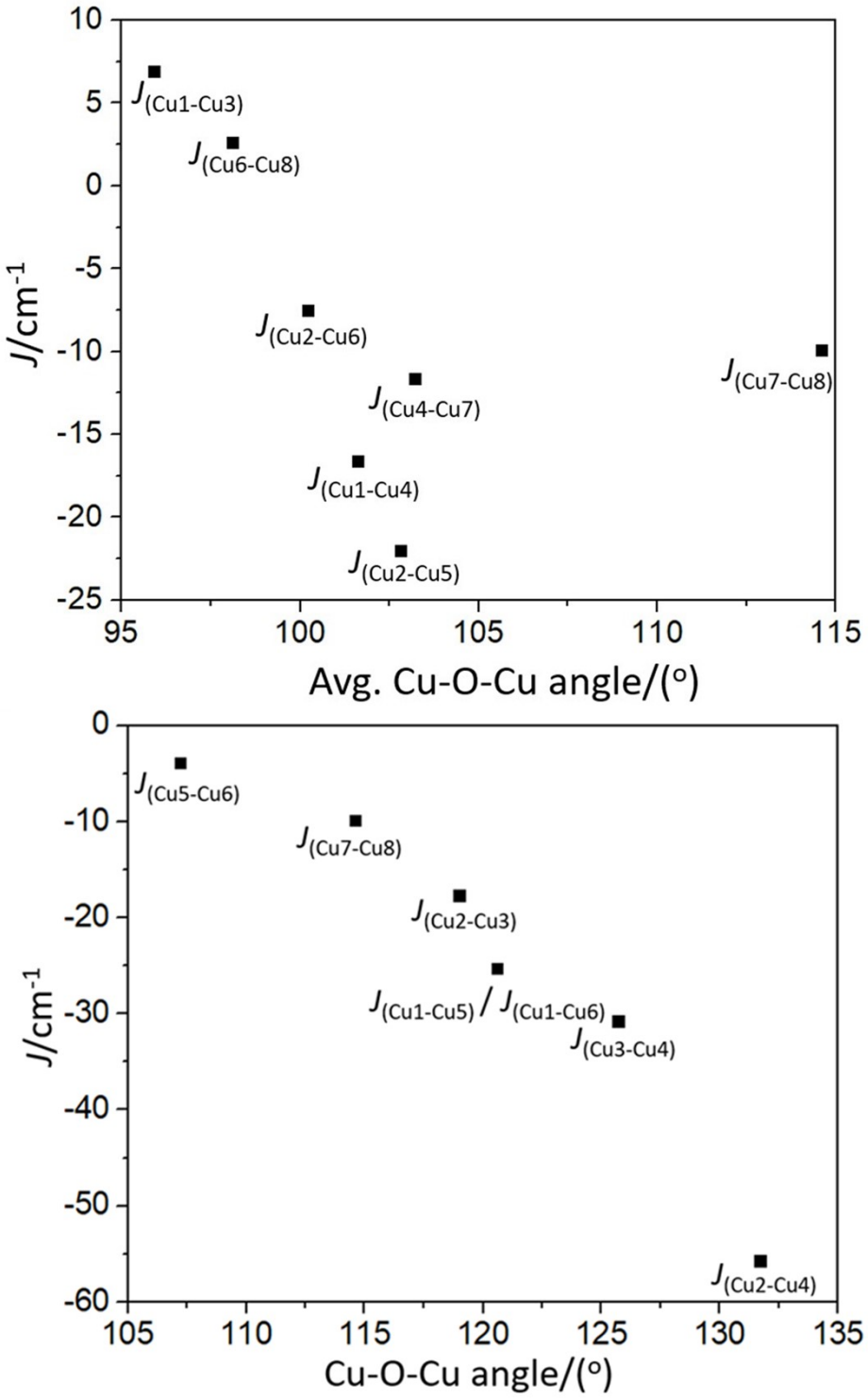

Figure S9. DFT estimated magnetic exchange interactions plotted versus the Cu-O-Cu angle (°) for pairs of nearest neighbour Cu ions in **4**. The upper graph shows Cu ions linked by two different bridging ligands, the lower graph shows Cu ions linked by one bridging ligand. The magneto-structural correlation reveals that the sign and magnitude of *J* strongly depends on the Cu-O-Cu angle, with larger Cu-O-Cu angles leading to strong antiferromagnetic exchange whose magnitude decreases with decreasing angle. The small deviation observed for $J_{(Cu4\text{-}Cu7)}$ is due to a counter-complementarity effect due to the presence of μ_2-OR/O(NO_2) groups. The deviation for $J_{(Cu7\text{-}Cu8)}$ is due to the near-negligible contribution to the exchange through the nitrate anion. This pathway therefore resembles a one ligand bridge and thus we include it in both plots. See the main text for details.

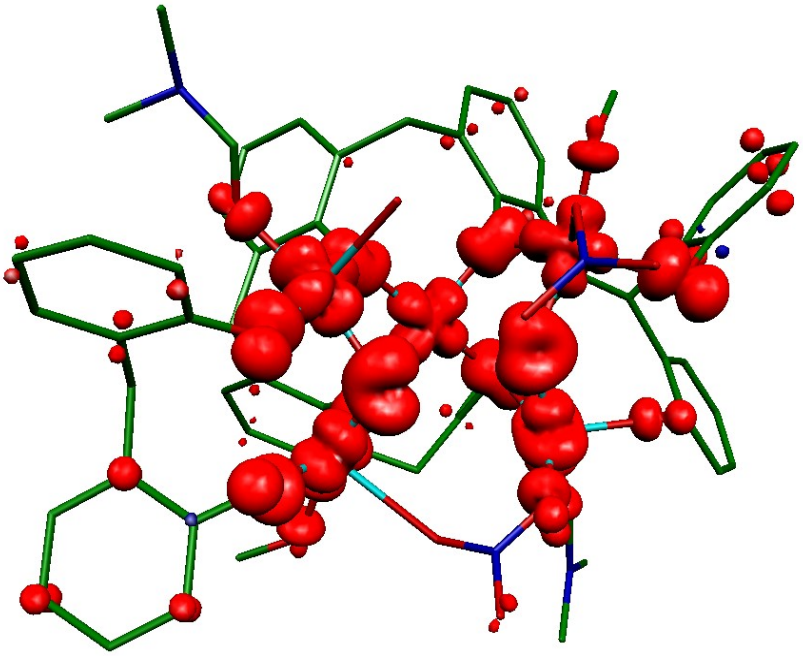

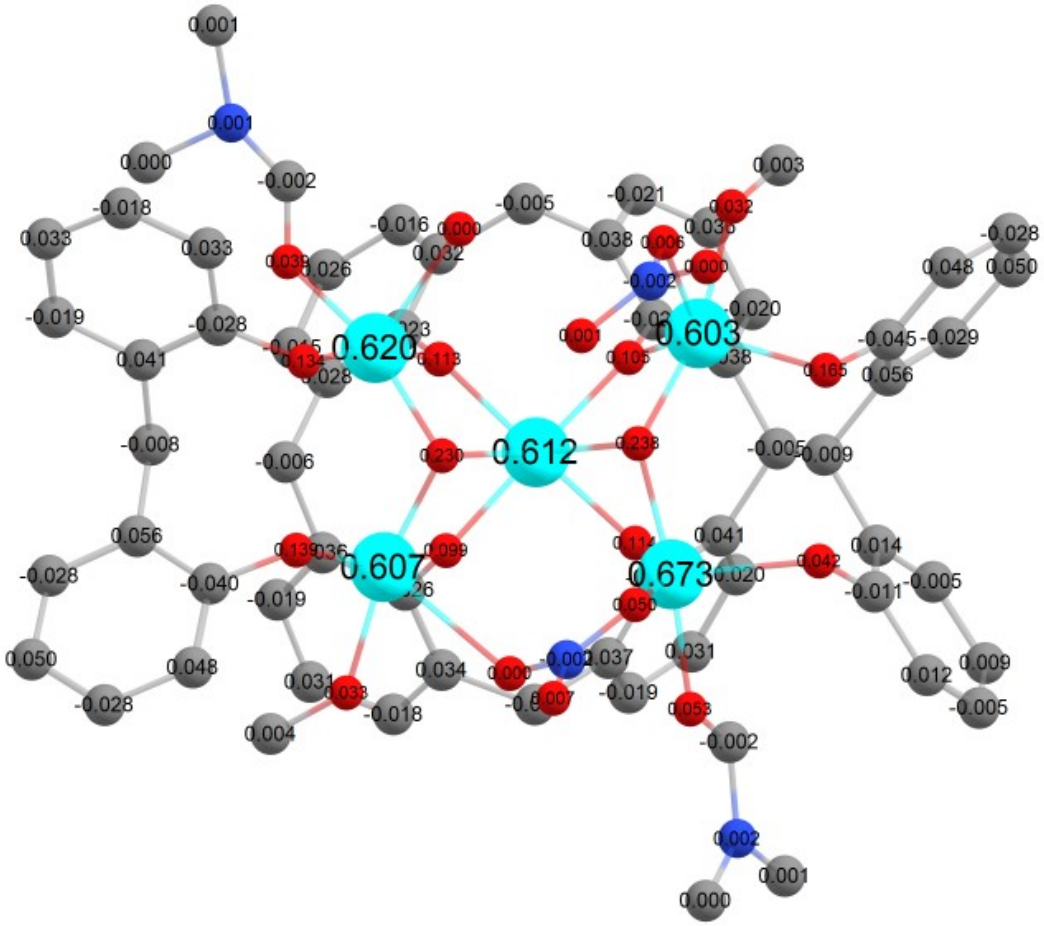
0.620
0.603
0.612
0.607
0.673

Figure S10. DFT estimated spin density plot (top) and values (bottom) for model **4A** with the isodensity surface value 0.003 e bohr^{-3}.

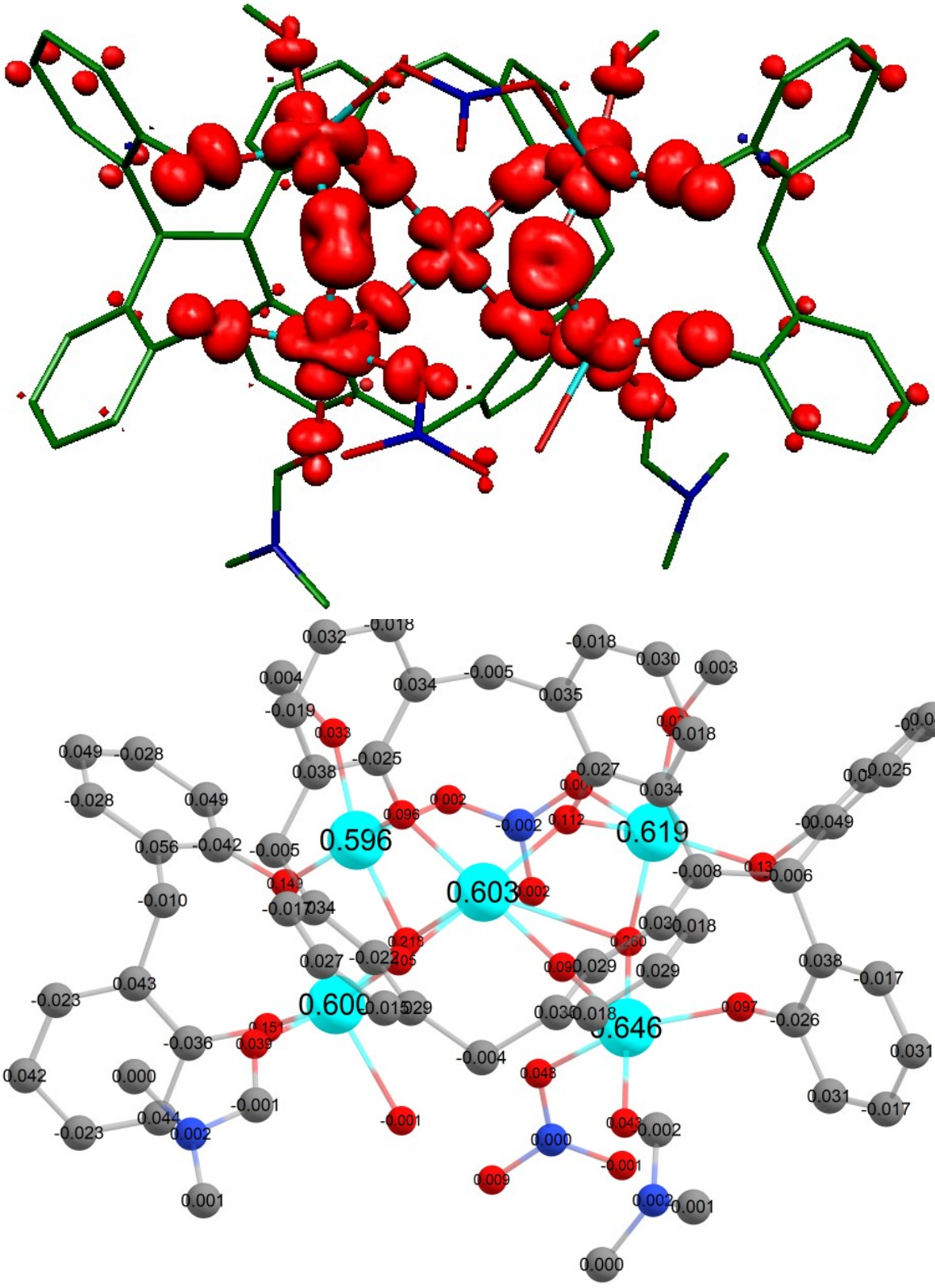
0.596
0.603
0.619
0.600
0.646

Figure S11. DFT estimated spin density plot (top) and values (bottom) for model **4B** with the isodensity surface value 0.003 e bohr^{-3}.

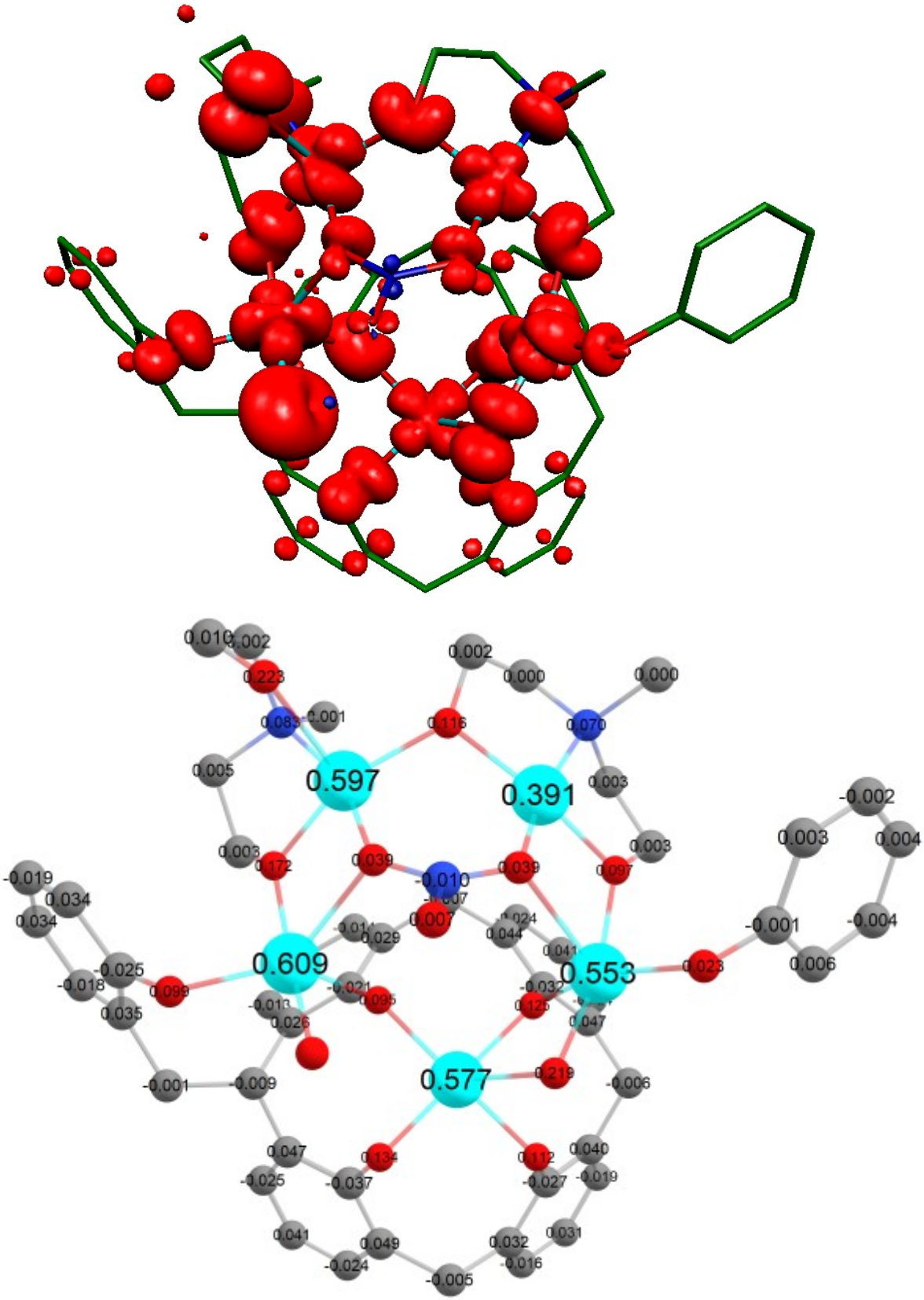

Figure S12. DFT estimated spin density plot (top) and values (bottom) for model **4C** with the isodensity surface value 0.003 e bohr^{-3}.

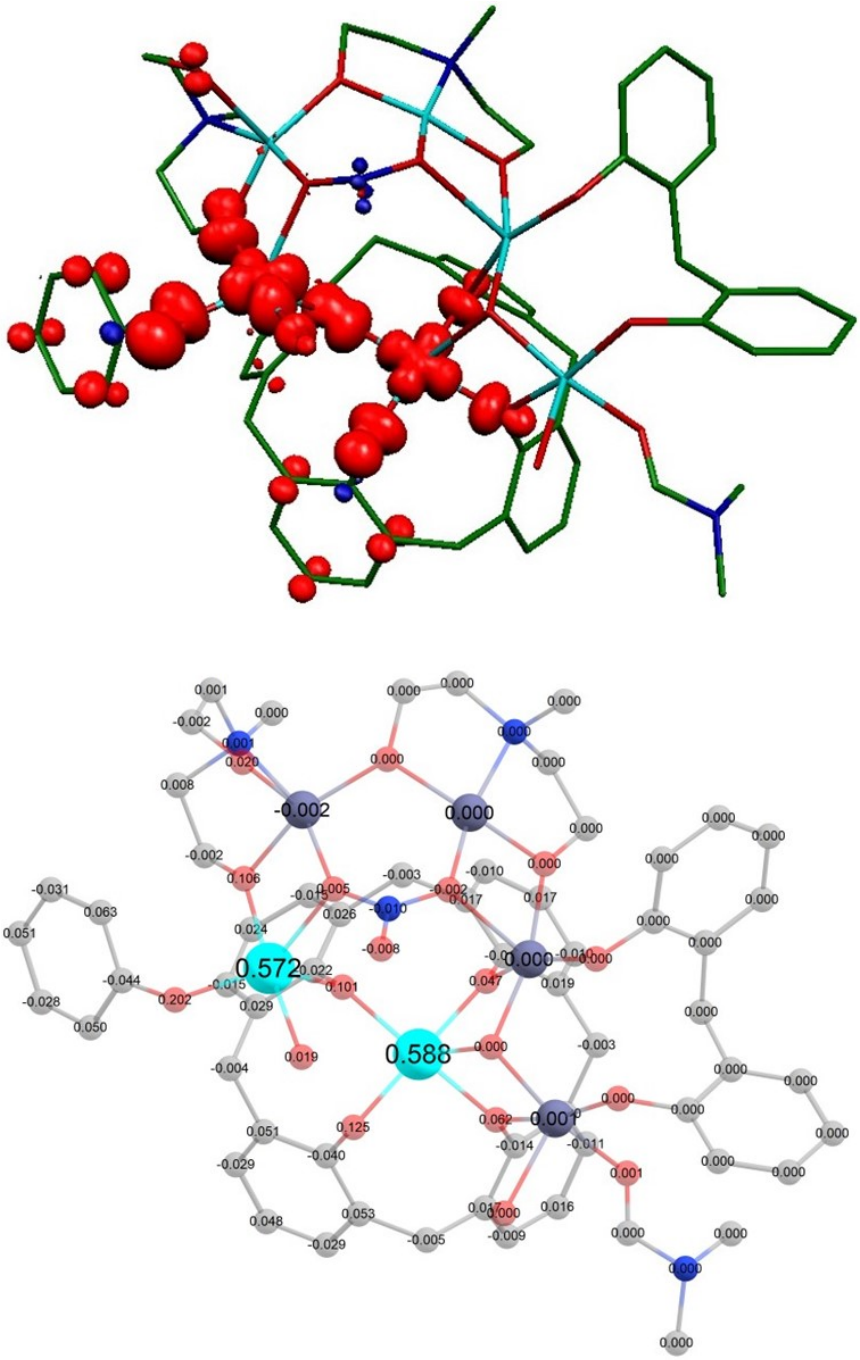

Figure S13. DFT estimated spin density plot (top) and values (bottom) for model **4D** with the isodensity surface value 0.003 e bohr^{-3}.

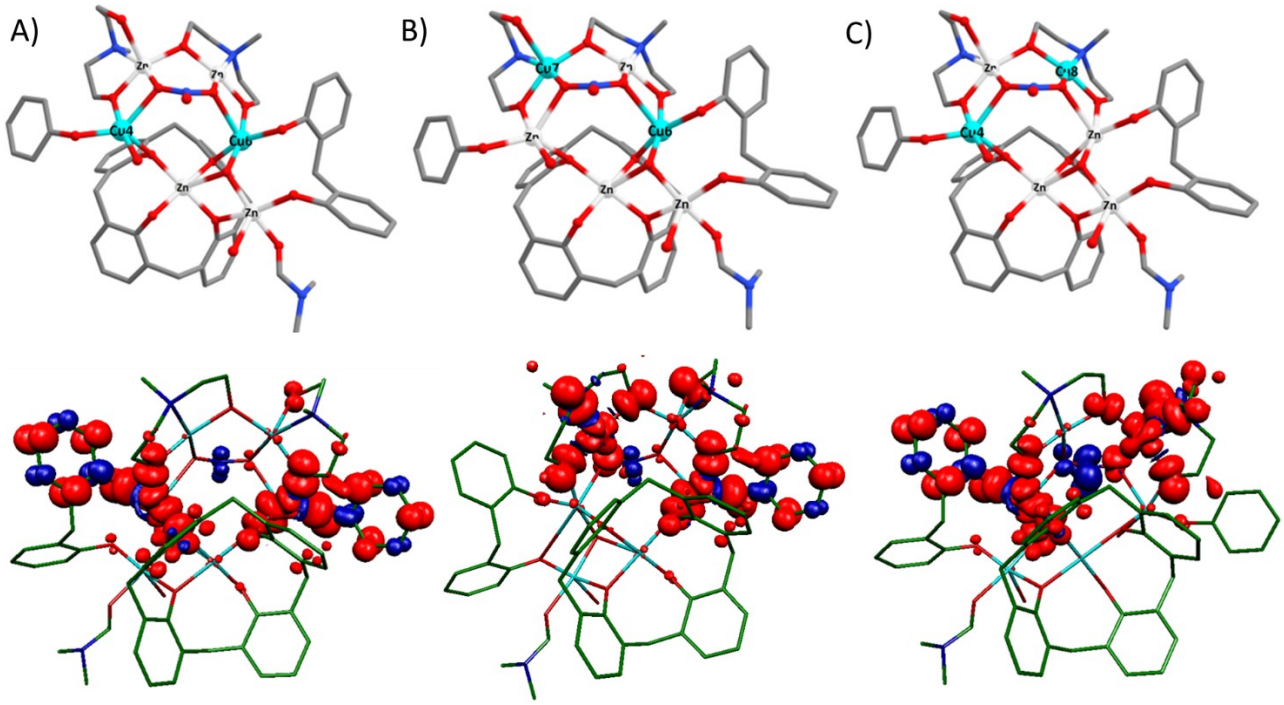

Figure S14. The three dimetallic model complexes (top) used to calculate the magnetic exchange interactions mediated solely through the nitrate anions between A) Cu4-Cu6, B) Cu7-Cu6 and C) Cu4-Cu8. The values are J = -0.6 cm^{-1}, +0.9 cm^{-1} and +0.8 cm^{-1}, respectively. The *syn, syn*-coordination mode ($J_{Cu4\text{-}Cu6}$) results in a weak antiferromagnetic exchange interaction and the *syn*, anti-coordination mode ($J_{Cu6\text{-}Cu7}$ and $J_{Cu4\text{-}Cu8}$) results in a weak ferromagnetic exchange interaction. The associated spin density plots are shown in the bottom half of the figure, with an isodensity surface value 0.001 e $bohr^{-3}$. The small spin densities evident on the N, O-atoms of the nitrate are indicative of weak magnetic exchange.